Int. J. Heat Mass Transfer. Vol. 34, No. 12, pp. 3075–3081, 1991
Printed in Great Britain

0017–9310/91 $3.00 + 0.00

Measurement of the local convection coefficient by pulsed photothermal radiometry

DAVID J. CROWTHER and JACQUES PADET
Groupe de Thermomécanique, Service Universitaire d'Energétique, GRSM, Faculté des Sciences de Reims, BP 347-51062 Reims Cedex, France

(*Received* 15 *June* 1990 *and in final form* 11 *January* 1991)

Abstract—Pulsed photothermal radiometry is used for the determination of the convection coefficient. The theoretical analysis of the transient wall temperature after a brief excitation is based on the use of the zero-order temporal moment. Different solutions to determine the convection coefficient from experimental thermograms are proposed and tested for insulating walls as well as conducting ones. Experimental results are compared to those given by a dissipation fluxmeter in order to validate the pulsed method.

INTRODUCTION

BASED on the Flash method introduced by Parker *et al.* [1] in 1961, pulsed photothermal radiometry is now a much used tool for non-destructive testing operations [2, 3] as well as measurement of thermophysical properties such as thermal diffusivity [4–6]. This photothermal method, initially used in transmission, is used by reflexion in its modern form, completely optical and without any contacts; excitation and detection are realized on the same side of the solid medium. The method consists of analysing the transient temperature on the front face of a wall, after a sudden deposit of luminous energy. Our work consists of an adaptation of this experimental principle to the detection and the measurement of the local convection coefficient. From a one-dimensional model of the wall temperature, taking into account its thermal nature (low or infinite thermal conductivity), we propose different methods for the transient analysis. Those methods rely on the notion of temporal moment [3, 7, 8] and in particular on the zero-order temporal moment. In order to validate the proposed solutions, we will compare the results obtained by the pulsed method with those given by a steady-state dissipation fluxmeter realized in this aim. The study has been realized in the case of forced convection between a fluid (air) and a wall. In steady state, the heat transfer is described by Newton's law: $\varphi = hS\Delta T$, in which h is a constant heat exchange coefficient (including convection and radiation exchanges).

THEORETICAL MODEL

We want to identify the heat exchange coefficient h from the evolution of the temperature of the front face of a wall, obtained after a brief thermal perturbation (Dirac). If we suppose that the energy deposit is uniformly distributed, we must solve the following linear model (Fig. 1):

$$\frac{\partial^2 T}{\partial x^2} - \frac{1}{a}\frac{\partial T}{\partial t} = 0$$

$$x = 0, \quad -\lambda\frac{\partial T}{\partial x} = h(T - T_a) - i(t)$$

$$x = e, \quad \frac{\partial T}{\partial x} = 0$$

$$t = 0, \quad T = T_a. \tag{1}$$

In equation (1), $i(t)$ is a known function describing the temporal distribution of the perturbation. In the case of a Dirac excitation of heat density Q, we obtain by Laplace transform the expression of the temperature's front face of a wall

$$\theta(0, t) = \frac{2Q}{\rho ce}\sum_{n=1}^{\infty}\frac{U_n^2}{Bi + Bi^2 + U_n^2}\exp\left(-\frac{U_n^2 at}{e^2}\right) \tag{2}$$

in which U_n is the nth-root of the transcendental equation: $U\tan(U) = Bi$.

In parallel to this model called 'finite thickness wall' we can define two particular cases, commonly used, from the behaviour of the wall (low or infinite thermal conductivity).

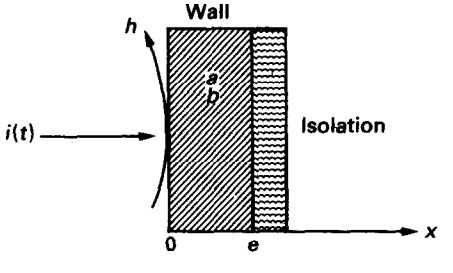

FIG. 1. Schematic description of the general model.

NOMENCLATURE

a thermal diffusivity, $\lambda/(\rho c)$ [$m^2 s^{-1}$]
b thermal effusivity, $\sqrt{(\lambda \rho c)}$ [$J m^{-2} °C^{-1} s^{-1/2}$]
c specific heat [$J kg^{-1} °C^{-1}$]
e thickness [m]
h superficial heat exchange coefficient [$W m^{-2} °C^{-1}$]
h_c convection coefficient [$W m^{-2} °C^{-1}$]
h_r radiation coefficient [$W m^{-2} °C^{-1}$]
m_0, m_{-1}, m_i zero-, minus one- and ith-order temporal moment
m_0^*, m_{-1}^*, m_i^* dimensionless zero-, minus one- and ith-order moment
Q heat flux [$J m^{-2}$]
R_{th} thermal resistance [$m^2 °C W^{-1}$]
T temperature [°C]
T_a ambient temperature [°C]
t time variable [s]
x space variable [m].

Dimensionless numbers
Bi Biot number, $(he)/\lambda$
Fo Fourier number, $(at)/e^2$
$Bi\sqrt{(Fo)}$ $(h\sqrt{t})/b$
$Bi\,Fo$ $(ht)/(\rho ce)$.

Greek symbols
α absorptivity
ε emissivity
θ temperature, $(T-T_a)$
θ_c wall temperature for a finite duration excitation [°C]
θ_d wall temperature for a Dirac excitation [°C]
λ thermal conductivity [$W m^{-1} °C^{-1}$]
ρ density [$kg m^{-3}$]
σ Planck constant, $5.67 \times 10^{-8} W m^{-1} °C^{-4}$
τ duration of the excitation [s]
τ_s system time constant [s]
φ_0 incident flux [$W m^{-2}$]
φ_c convection flux [$W m^{-2}$]
φ_r radiation flux [$W m^{-2}$]
φ_p rear flux [$W m^{-2}$]

(a) Low conductivity walls can be described by a 'semi-infinite wall' model defined in our case by

$$\theta(0,t) = \frac{Q}{b\sqrt{(\pi t)}}\left\{1 - \frac{h}{b}\sqrt{(\pi t)}\exp\left[\left(\frac{h}{b}\right)^2 t\right]\operatorname{erfc}\left(\frac{h}{b}\sqrt{t}\right)\right\} \quad (3)$$

in which erfc (x) is the complementary error function.

(b) In the second case, because of the infinite nature of the thermal conductivity, we can consider that at any time the temperature is uniform inside the wall; so it only depends on the time variable. This model, called 'isothermal thin wall', is described by

$$\theta(t) = \frac{Q}{\rho ce}\exp\left(-\frac{ht}{\rho ce}\right). \quad (4)$$

Expressions (3) and (4) present the advantage of being more simple to use than expression (2), while they describe many practical cases in a very satisfactory way. We can easily extend those models to the case of a finite duration τ excitation, by application of Duhamel's theorem

$$\theta_c(0,t) = \int_0^t \theta_d(0, t-u)\phi(u)\,du \quad (5)$$

with

$$\text{if } t > \tau, \quad \phi(u) = 0$$
$$\text{if } t < \tau, \quad \phi(u) = 1/\tau.$$

For more details concerning all the calculations see ref. [8]. From expressions (2)–(4), we can calculate the dimensionless wall temperature vs the Fourier number, for different Biot numbers in the case of a 'finite thickness wall' model (Fig. 2), or vs the grouping $Bi\sqrt{(Fo)}$ or $Bi\,Fo$, for the 'semi-infinite wall' model and the 'isothermal thin wall' model, respectively (Figs. 3 and 4).

IDENTIFICATION OF THE h COEFFICIENT

Principle

The proposed solutions for the identification of the h coefficient from the transient wall temperature rest on the use of the zero-order temporal moment defined by

$$m_0 = \int_0^{+\infty} \theta(u)\,du. \quad (6)$$

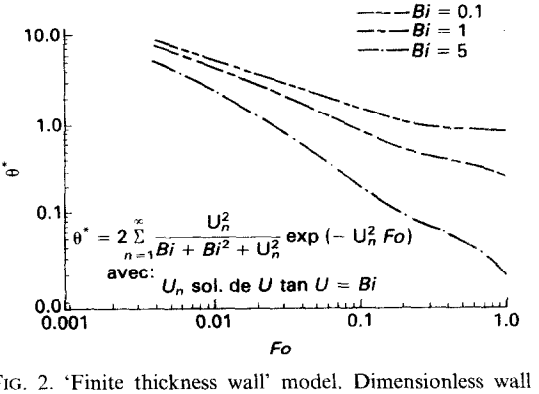

FIG. 2. 'Finite thickness wall' model. Dimensionless wall temperature vs Fourier number.

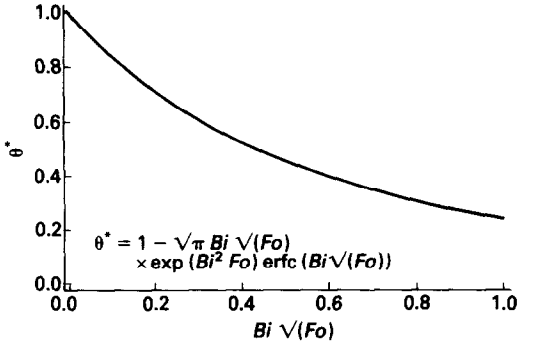

FIG. 3. 'Semi-infinite wall' model. Dimensionless wall temperature vs $Bi\sqrt{(Fo)}$.

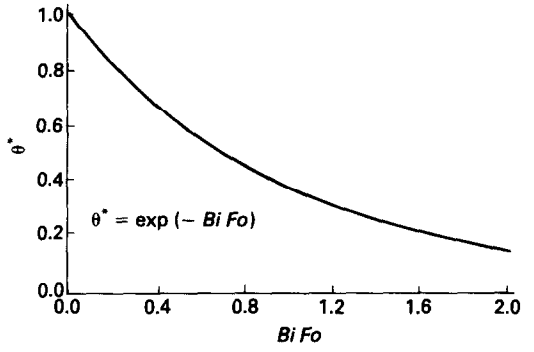

FIG. 4. 'Isothermal thin wall' model. Dimensionless wall temperature vs $Bi\,Fo$.

The quantity m_0 is very interesting because it is representative of the heat exchange between the wall and the fluid; we can show [7] for the 'semi-infinite wall' model and the 'isothermal thin wall' model that we have $m_0 = Q/h$. The lower the value of h, the slower the integral converges; so because of the finite duration of the experimental thermograms, we must introduce a partial zero-order temporal moment defined by

$$m_0 = \int_0^{t_f} \theta(u)\,\mathrm{d}u \tag{7}$$

in which t_f is the total duration of the thermogram.

The integral presents the double advantage of taking into account the total information of the thermogram, and of eliminating the noise if its average value is equal to zero during the interval studied. From definition (7) and for models (3) and (4), we propose different solutions for determining the h coefficient.

'Semi-infinite wall'

Experimentally, we have not one, but two unknown quantities: h and the energy term Q. The value of Q is hard to find; we must consequently eliminate or calculate it. Its elimination can easily be realized by dividing the experimental wall temperature by its maximum (normalization of the thermogram). When this is impossible, it is necessary to calculate it from a suitable analytical model. Knowing this, we propose two ways to determine h.

(a) The first solution, called 'direct identification', consists, from the analytical model, of searching numerically for the theoretical value of h giving the equality between the experimental and the theoretical partial zero-order moment.

(b) The second solution relies on a correlation. Knowing that for an adequate time, the zero-order temporal moments of a 'semi-infinite wall' are equal for a Dirac or a finite duration excitation, we determine a relation between a dimensionless moment (m_0^*) and the grouping $Bi\sqrt{(Fo)}$

$$f(m_0^*) = 5.48 - 13.53m_0^* + 12.39(m_0^*)^2 - 4.19(m_0^*)^3$$

with

$$f(m_0^*) = Bi\sqrt{(Fo)}. \tag{8}$$

This relation has been established numerically from values calculated by the model. So we have

$$h = \frac{b}{\sqrt{t}} f(m_0^*)$$

with

$$m_0^* = \frac{m_0(t)b}{Q\sqrt{t}}. \tag{9}$$

'Isothermal thin wall'

In that case we envisaged three solutions.

(a) For the first one, because of the extreme simplicity of the model (4), we can realize an exponential regression (by a least square method) on the experimental thermogram. The result of the regression $[\theta(t) = \exp(A)\exp(Bt)]$ is identified with (4) to obtain

$$Q = \rho ce \exp(A)$$
$$h = -\rho ceB. \tag{10}$$

We notice that the principal advantage of this method, besides its rapidity, is to determine both unknown quantities of our system at the same time. However, for poor quality thermograms in particular, we can obtain a regression curve quite different from the experimental one. To avoid this, we add to the regression one condition on the experimental area. By adjusting the boundaries of the regression we search the regression curve which keeps the experimental area. This condition allows us to find the most representative exponential of the experimental evolution.

(b) The second method uses a correlation established in the same way as the 'semi-infinite wall' model. This time, from expression (4), we obtain a relation between a dimensionless moment (m_0^*) and the grouping $Bi\,Fo$:

$$g(m_0^*) = 7.3 - 18.93m_0^* + 18.58(m_0^*)^2 - 6.92(m_0^*)^3$$

with

$$g(m_0^*) = Bi\,Fo \tag{11}$$

which leads to

$$h = \frac{\rho ce}{t} g(m_0^*)$$

with

$$m_0^* = \frac{m_0(t)\rho ce}{Qt}. \tag{12}$$

(c) At last, from the analytical expression of the ith-order temporal moment of expression (4), we obtain the relation

$$m_i = \tau_s m_i^* \tag{13}$$

in which m_i^* is the ith-order dimensionless moment. In particular, for the -1 and 0 order we have

$$m_0 = \tau_s m_0^*$$
$$m_{-1} = m_{-1}^*. \tag{14}$$

So, from the -1 and 0 order experimental temporal moments, knowing the relation between the -1 and 0 order dimensionless moments (called identification function F), we can easily find h by

$$h = \rho ce \frac{F(m_{-1}^*)}{m_0}. \tag{15}$$

The F-function has been approached for normalized thermograms from theoretical values of the -1 and 0 order dimensionless moments

$$m_0^* = -3.756 + 2.237m_{-1}^* - 0.265(m_{-1}^*)^2. \tag{16}$$

EXPERIMENTAL WORK

Experimental device

We realized an experimental device (Fig. 5) for the local acquisition of the temperature's front face of a wall after a deposit of luminous energy. It can be shared in three parts.

(a) An excitation part composed of a continuous YAG laser (1.06 μm), mechanically modulated by a metallic strip stuck onto a speaker. A function generator controls the motion of the speaker, so that we can generate excitations of any duration. In addition, a lens permits us to obtain on the wall a spot large enough to consider that in its centre the thermal phenomenon is one-dimensional.

(b) The second part collects the infra-red radiations emitted by the wall. It is composed of a first mirror which collects a part of the infra-red radiations and sends them to a HgCdTe detector through a second mirror.

(c) A data acquisition part, is composed of an analogical/digital sampler controlled by a microcomputer and a function generator. An oscilloscope permits the visualization in real time of the signal given by the detector.

The exchange condition is realized by sending air, colder than the ambience, to the wall's front face.

Experimental results

We choose to test the different solutions proposed for the h determination on two types of material: metals and insulating materials.

Insulating wall. The insulating wall is a 2.5 mm thick plastic sample ($a = 1.13 \times 10^{-7}$ m^2 s^{-1}, $b = 514$ J m^{-2} K^{-1} s$^{-1/2}$). We realize the acquisition of the local transient temperature of the sample for three air flows ($U_1 \cong 1.5$ m s^{-1}, $U_2 = 2U_1$ and $U_3 = 3U_1$). The acquisition duration was 26 s for a 1 s excitation. We present in Fig. 6 the experimental thermograms and in Fig. 7 the evolution of their partial zero-order temporal moment. In Fig. 6 there is quite good differentiation of the superficial exchange rates. However, it is much more obvious in Fig. 7 by the application of the temporal moment. We present in Table 1 the calculated h values for the experimental thermograms. There is quite good convergence of the results given by both methods, despite their fundamental differences.

Metallic wall. We used a 1 mm thick aluminium sample ($a = 0.86 \times 10^{-4}$ m^2 s^{-1}, $b = 21550$ J m^{-2} K^{-1} s$^{-1/2}$). We present in Fig. 8 the transient wall temperatures for a free convection and a forced convection with their respective regression curves, and their partial zero-order temporal moment (Fig. 9). We notice that despite a low signal-to-noise ratio (Fig. 8), the partial zero-order temporal moment gives a very good differentiation of the exchange rates. We verify, in this case, the great utility of the zero-order temporal moment. Table 2 shows the calculated h values given by the proposed methods. We notice this time a quite important divergence in the free convection case. We must say that in both cases studied (insulating wall and metallic wall), the free convection results must be regarded with caution, because as the absolute measurement error is quite constant, the lower the value of h, the higher the relative error committed. In forced convection, results are more convergent, considering the poor quality of the thermograms.

Time evolution of h. The previous calculations have been realized at time $t = 26$ s (i.e. at the end of the acquisition interval). If we do the same calculations at different times of the thermograms, we verify that the h coefficient does not remain constant during the pulsed experiment (Fig. 10): it goes from an extreme to an asymptotic value. That fact is in accordance with the theoretical analysis made in ref. [10]. We can show that this asymptotic value is representative of the established steady state. Consequently, to obtain the h-value of the steady state, we must realize the calculations for a time as long as possible, i.e. at least equal to the experimental interval.

Radiation losses linearization. We suppose that h is

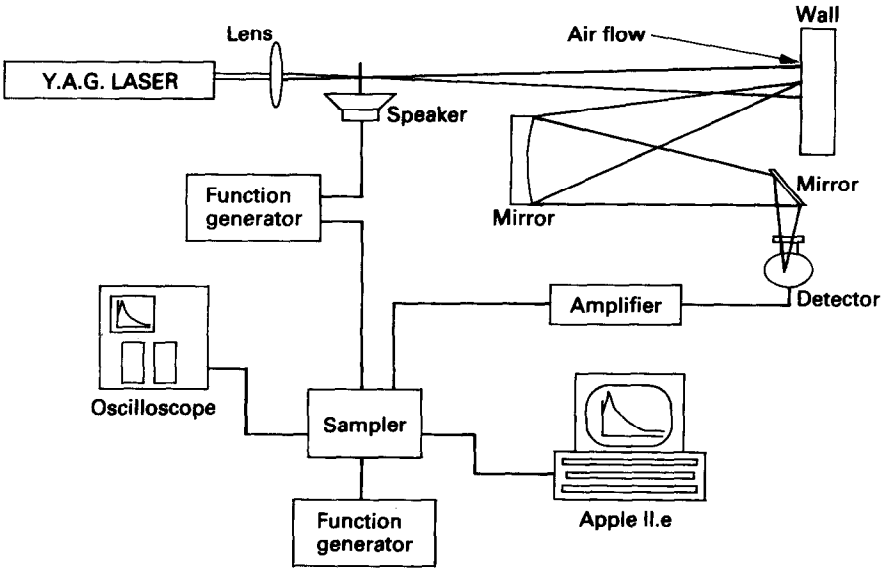

FIG. 5. Experimental device. Acquisition of the local wall i.r. radiation.

the sum of two coefficients: an h_c coefficient (convection losses) and an h_r coefficient (radiation losses). Knowing h, we must determine h_r to find finally the convection coefficient. To this aim, we linearize the radiative transfer equation [11]: $\varphi_r = \varepsilon\sigma(T^4 - T_a^4)$.

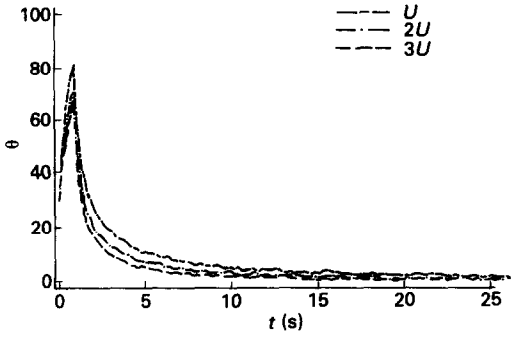

FIG. 6. Insulating wall. Experimental thermograms.

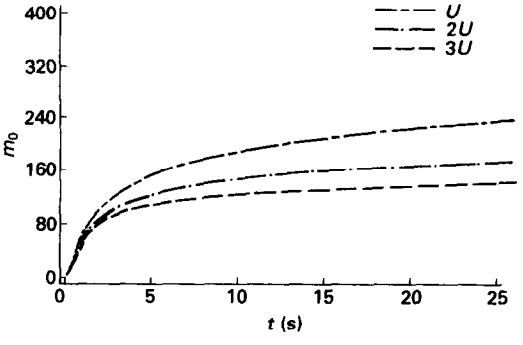

FIG. 7. Insulating wall. Zero-order partial moments of the experimental thermograms.

This equation can be written in the same way as Newton's law: $\varphi_c = h_c(T - T_a)$ with

$$h_r = \varepsilon\sigma(T^2 + T_a^2)(T + T_a). \tag{17}$$

So, we can now find easily an average value of h_r and calculate the convection coefficient by: $h_c = h - h_r$.

Experimental validation of the pulsed method

In order to validate the pulsed method, we decided to compare it to another well-known measurement method. We realized in this aim a steady-state dissipation fluxmeter [12]. The principle is as follows: we insulate a volume element in a wall. This element and

Table 1. Experimental values of h for three different air flows, case of the insulating wall (h in W m^{-2} °C^{-1})

	Correlation	Direct identification
U_1	69	72
U_2	121	103
U_3	158	152

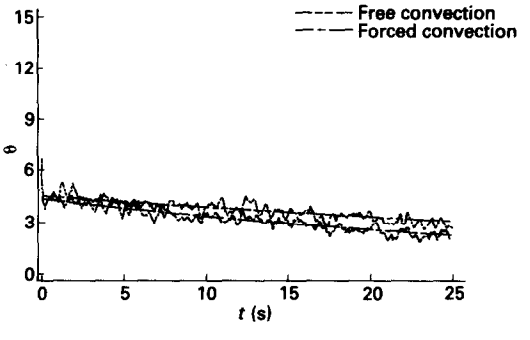

FIG. 8. Conducting wall. Experimental thermograms.

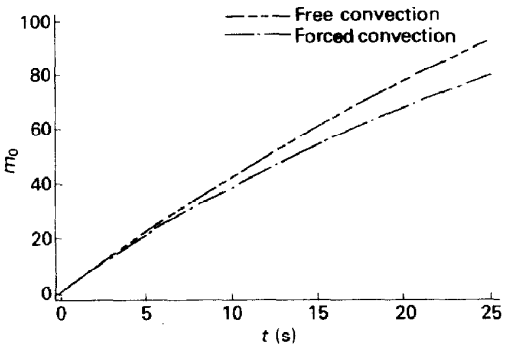

FIG. 9. Conducting wall. Zero-order partial moments of the experimental thermograms.

Table 2. Experimental values of h for two different exchange rates, case of the metallic wall (h in W m^{-2} °C^{-1})

	Regression	Correlation	Identification function
Free convection	35	23	13
Forced convection	60	60	50

the wall are heated up in a separated way, to obtain a uniform wall temperature. When this equilibrium is obtained, if we know the thermal power dissipated in the volume element, from the conservation heat equation (18), we find the expression of the convection coefficient (19)

$$\alpha\varphi_0 = \varphi_r + \varphi_c + \varphi_p \tag{18}$$

$$h_c = \frac{1}{(T - T_a)}\left[\alpha\varphi_0 - \varepsilon\sigma(T^4 - T_a^4) - \frac{T - T_a}{R_{th}}\right]. \tag{19}$$

Our fluxmeter has been made in the following way: the wall of the fluxmeter is made with a 200 × 300 × 5 mm aluminium plate, in which we had implanted a measurement element composed of an aluminium chip (diameter = 10 mm, thickness = 1 mm) stuck

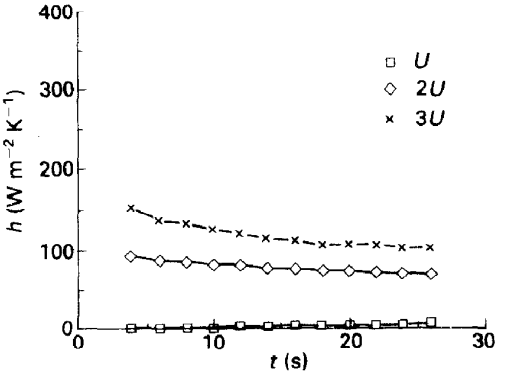

FIG. 10. Insulating wall. Evolution of the calculated h-values vs time. Calculation by direct identification method.

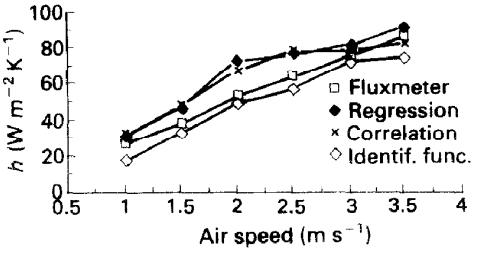

FIG. 11. Conducting wall. Comparison of the three proposed methods and the fluxmeter method.

onto a PVC cylinder (diameter = 10 mm, thickness = 5 mm). This element is positioned in the fluxmeter plate by three silicon dots. The measurement element is insulated from the wall by a 1 mm thick ring of air. The plate is heated up on its rear face by an electrical resistance, and the measurement element on its front face by a laser beam. The whole thing is insulated on the back face by a 2.5 cm thick layer of glass wool, to limit the heat losses as much as possible. The control of the wall temperature uniformity is realized by an i.r. video camera. This allows us to adjust the laser beam power at any time. With this experimental device, we realized measurements by the pulsed method and by the fluxmeter method at the same time, for different air flows on the front side of the wall. As the plate is made of aluminium we must use the 'isothermal thin wall' model to describe its thermal evolution. We made measurements for six different air flows (≅ 1, 1.5, 2, 2.5, 3 and 3.5 m s^{-1}). We present in Fig. 11 the results given by each method. Despite the difference between the solutions proposed for the h determination and besides the quite poor quality of the experimental thermograms in the case of conducting materials (e.g. Fig. 8), the results given by all the methods are quite convergent, which is very encouraging for the use of the transient method.

CONCLUSION

We have shown that, by means of a pulsed photothermal radiometry method, it is possible to detect a superficial heat exchange and thus to calculate a convection coefficient. The method is quite efficient in forced convection, but not yet precise enough to envisage measurement in free convection, besides the use of zero-order temporal moments. However, completely optical and without any contacts, this method can be useful for some control operations realized *in situ*. We verified that the exchange coefficient is not constant during the pulsed experiment, but finally we found that this is not a real handicap to find an h value representative of a steady-state heat exchange.

REFERENCES

1. W. J. Parker, R. J. Perkins, C. P. Butler and G. L. Abbott, Flash method for determining thermal diffu-

sivity, heat capacity and thermal conductivity, *J. Appl. Phys.* **32**, 1679–1684 (1961).
2. M. Heuret, E. van Schel, M. Egee and R. Danjoux, Bounding analysis of layered materials by photothermal radiometry, *Proc. Symp. EMRS Conf.*, Strasbourg, France (1989).
3. D. Boscher, A. Deom, G. Gardette and D. Balageas, Thermal NDT of carbon epoxy laminates, *Proc. Eurotherm 4*, Nancy, France, 28 June–1 July (1988).
4. A. Degiovanni, Contribution à l'étude de la diffusivité thermique, Thesis, University of Lyon, France, No. 75-19 (1975).
5. R. Danjoux, Radiométrie photothermique sous excitation pulsée, application à des matériaux composites et à des tôles d'acier émaillées, Thesis, University of Reims, France (1988).
6. D. Balageas, Thermal diffusivity measurement by pulsed methods, *High Temp.–High Pressure* **21**, 85–96 (1989).
7. D. Balageas et D. Boscher, L'évaluation des pertes dans les expériences photothermiques impulsionnelles. Application à la détermination des coefficients de transfert convectif sur des maquettes en soufflerie, *C. R. Acad. Sci. Ser. II* **305**, 13–16 (1987).
8. A. Degiovanni, Identification de la diffusivité thermique par l'utilisation des moments temporels partiels, *High Temp.–High Pressure* **17**, 683–689 (1985).
9. D. Crowther, Etude et développement d'une méthode optique pour la mesure des coefficients de convection, Thesis, University of Reims, France (1990).
10. J. Padet et P. Pierson, Evaluation des transferts thermoconvectifs en régime instationnaire. Approche théorique et expérimentale, *Revue Gen. Thermique* **287**, 781–788 (1985).
11. A. B. De Vriendt, *La transmission de la chaleur*, Vol. 1. Gaëtan Morin, Québec (1982).
12. H. Cordier, Une nouvelle méthode de mesure des coefficients locaux de convection, PST Ministère de l'air, NT 73 (1958).

MESURE LOCALE DU COEFFICIENT DE CONVECTION PAR RADIOMÉTRIE PHOTOTHERMIQUE IMPULSIONNELLE

Résumé—La radiométrie photothermique impulsionnelle est ici utilisée pour la détermination de coefficients de convection. L'analyse théorique du régime transitoire de la température pariétale suivant une excitation brève est basée sur l'utilisation des moments temporels d'ordre zéro. Différentes solution pour déterminer le coefficient de convection à partir de thermogrammes expérimentaux sont proposées et testées tant pour des parois isolantes que conductrices. Les résultats expérimentaux sont comparés à ceux donnés par un fluxmètre à dissipation, dans le but de valider la méthode impulsionnelle.

MESSUNG DES ÖRTLICHEN WÄRMEÜBERGANGSKOEFFIZIENTEN BEI KONVEKTION MIT HILFE DER GEPULSTEN PHOTOTHERMISCHEN RADIOMETRIE

Zusammenfassung—In der vorliegenden Arbeit wird die gepulste photothermische Radiometrie zur Bestimmung der Wärmeübergangskoeffizienten bei Konvektion verwendet. Die theoretische Untersuchung der transienten Wandtemperatur nach einer kurzen Anregung beruht auf der Verwendung des zeitlichen Moments nullter Ordnung. Es werden verschiedene Lösungen zur Bestimmung des Wärmeübergangskoeffizienten bei Konvektion aufgrund der experimentell ermittelten Thermogramme vorgeschlagen. Diese werden für isolierende Wände wie auch für leitende Wände überprüft. Die Versuchsergebnisse werden mit solchen verglichen, welche sich bei Verwendung eines Dissipationsstrommeßgerätes ergeben. Dies geschieht, um das Impulsverfahren zu bestätigen.

ОПРЕДЕЛЕНИЕ ЛОКАЛЬНЫХ ХАРАКТЕРИСТИК КОНВЕКЦИИ МЕТОДОМ ИМПУЛЬСНОЙ ФОТОТЕРМИЧЕСКОЙ РАДИОМЕТРИИ

Аннотация—Импульсная фототермическая радиометрия используется для определения характеристик конвекции. Теоретическое определение нестационарной температуры стенки после непродолжительного возбуждения базируется на использовании момента нулевого порядка. Предложены и апробированы различные способы определения характеристик конвекции на основе экзпериментальных термограмм для изолированных и проводящих стенок. С целью проверки эффективности импульсного метода экспериментальные данные сравниваются с результатами, полученными с использованием флюксметра.